Accepted Manuscript

Robust L-Malate bienzymatic biosensor to enable the on-site monitoring of malolactic fermentation of red wines

Pablo Giménez-Gómez, Manuel Gutiérrez-Capitán, Fina Capdevila, Anna Puig-Pujol, Cesar Fernández-Sánchez, Cecilia Jiménez-Jorquera

PII: S0003-2670(16)31411-8

DOI: 10.1016/j.aca.2016.11.061

Reference: ACA 234932

To appear in: *Analytica Chimica Acta*

Received Date: 21 June 2016

Revised Date: 2 November 2016

Accepted Date: 29 November 2016

Please cite this article as: P. Giménez-Gómez, M. Gutiérrez-Capitán, F. Capdevila, A. Puig-Pujol, C. Fernández-Sánchez, C. Jiménez-Jorquera, Robust L-Malate bienzymatic biosensor to enable the on-site monitoring of malolactic fermentation of red wines, *Analytica Chimica Acta* (2017), doi: 10.1016/j.aca.2016.11.061.

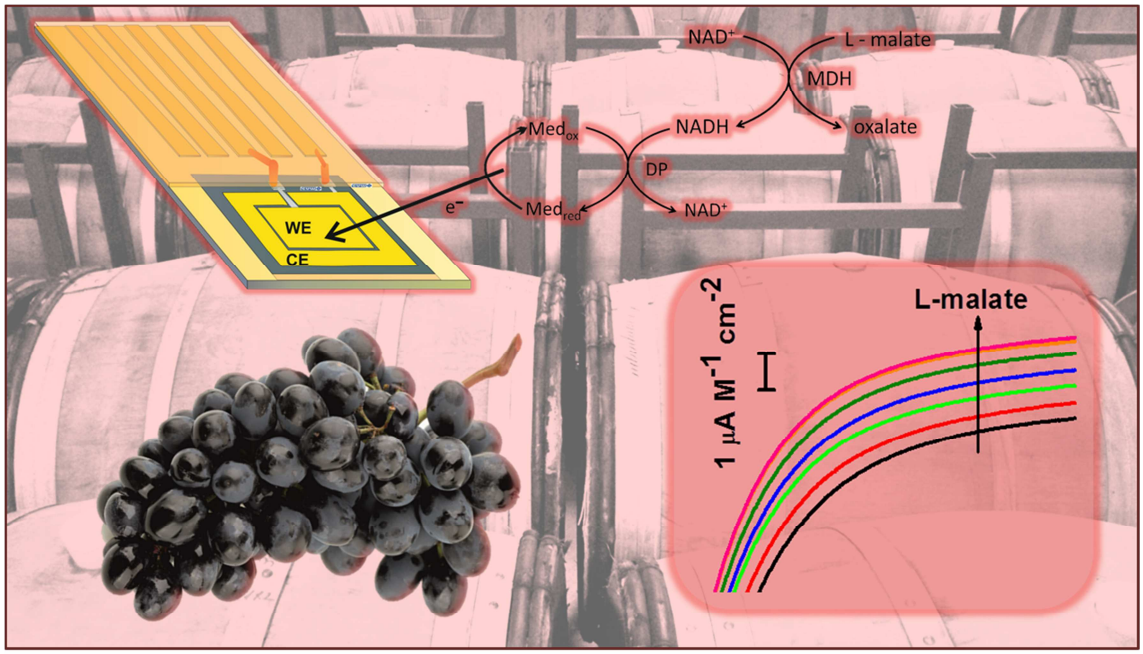

ROBUST L-MALATE BIENZYMATIC BIOSENSOR TO ENABLE THE ON-SITE MONITORING OF MALOLACTIC FERMENTATION OF RED WINES

Author for correspondence:

Dr. Manuel Gutiérrez-Capitán
Instituto de Microelectrónica de Barcelona (IMB-CNM), CSIC
Campus de la UAB
08193 Bellaterra, Barcelona
SPAIN

Tel +34 93 594 7700
Fax +34 93 580 0267
E-mail: manuel.gutierrez@csic.es

The total number of pages is (excluding this one): 31

ROBUST L-MALATE BIENZYMATIC BIOSENSOR TO ENABLE THE ON-SITE MONITORING OF MALOLACTIC FERMENTATION OF RED WINES

Pablo Giménez-Gómez[a], Manuel Gutiérrez-Capitán[a*], Fina Capdevila[b], Anna Puig-Pujol[b], Cesar Fernández-Sánchez[a] and Cecilia Jiménez-Jorquera[a]

[a] *Instituto de Microelectrónica de Barcelona (IMB-CNM), CSIC, Campus UAB, 08193 Bellaterra, Spain*

[b] *Institut Català de la Vinya i el Vi (IRTA-INCAVI), Plaça Àgora 2, 08720 Vilafranca del Penedès, Spain*

[*] *Corresponding author:* Manuel Gutiérrez-Capitán, *email: manuel.gutierrez@csic.es*

Abstract

Monitoring the malolactic fermentation process is strictly required to guarantee the sensorial quality and freshness of red wines. This could be achieved by in-field and real-time continuous measurements of L-malate concentration in the fermentation tanks. The potential of a miniaturized amperometric bienzymatic biosensor as an analytical tool to be applied in such scenario is described in this paper. The biosensor comprises a thin-film gold electrode as transducer, malate dehydrogenase (MDH) and diaphorase (DP) enzymes together with nicotinamide adenine dinucleotide (NAD^+) cofactor as the selective receptor and an adequate redox mediator to record the corresponding amperometric signal. Three different biosensor architectures are studied, whose main differences lie in the immobilization of the different chemical components onto the electrode surface. In all cases a fast-electrosynthethized polypyrrole (PPy) membrane is generated for this purpose. The experimental conditions are optimized an the best

architecture shows a sensitivity of 1365±110 mA M^{-1} cm^{-2} and a detection limit of 6.3×10^{-8} M in a concentration range of 1×10^{-7} M – 1×10^{-6}M. The biosensor presents an excellent working stability as it retains above 90 % of its sensitivity after 37 days, thus enabling the monitoring of the malolactic fermentation of three red wines. The obtained results show excellent agreement with the standard colorimetric method.

Keywords: Amperometric bienzymatic biosensor; Electrosynthesized polypyrrole membrane; Immobilization of redox mediator; L-malic acid analysis; Malolactic fermentation

1. Introduction

L-malic acid is one of the principal organic acids in grapes [1]. It is mainly synthesized via glycolysis and its concentration depends on the climatic conditions and temperature during harvesting and crushing of the grapes [2]. However, the presence of L-malic acid affects the final quality of the wine by deteriorating its biochemical and microbial stability, and hence its sensorial quality and freshness. This is why an adjustment of the acidity is performed in red wines by malolactic fermentation (MLF), wherein the L-malic acid, in a concentration of 1 - 3 g L^{-1} (7.5×10^{-3} – 2.2×10^{-2} M), is converted to L-lactic acid and CO_2 by lactic acid bacteria action [3]. During alcoholic fermentation, yeast strain converts grape sugars, glucose and fructose, into ethanol. Once these sugars are consumed, the yeast concentration decreases and the lactic acid bacteria (LAB) perform the malolactic fermentation using the malolactic enzymes [4]. Natural or induced malolactic fermentation is carried out in the production of all red wines.

The conventional analytical methods for the determination of L-malic acid in wine are chromatography [5-7] and electrophoresis [8, 9]. These methods require the use of bulky expensive equipment and are time consuming. Alternative enzymatic approaches based on the detection of nicotinamide adenine dinucleotide (NADH) by absorbance were also reported [10]. In them, L-malic acid is oxidized to oxaloacetate in presence of NAD^+ and catalyzed by L-malate dehydrogenase (L-MDH) enzyme. Then, the produced NADH is detected by absorbance at 340 nm and stoichiometrically related to the L-malic acid in the sample. However, this procedure has to be carried out in an external laboratory and is reagent consuming. The application of biosensors for in-field determination of malic acid appears to be an excellent option for the strict and continuous control of this fermentation process. These are based on different enzymatic approaches [11-15], but the most applied one makes use of a cascade bienzymatic reaction involving the catalytic reactions of L-MDH enzyme in the presence of NAD^+ as co-factor, and consecutively of Diaphorase (DP) enzyme coupled to an appropriate redox mediator. The readout of this reaction can be carried out by spectrophotometry [16] or amperometry [17, 18].

In this work, the potential of an amperometric biosensor for in-field detection of L-malate is presented. Amperometric biosensors are characterized by its small size, low manufacturing costs, potential portability for in-situ analysis, low volume reagent consumption, wide linear response range and high selectivity and reproducibility [19]. Different redox mediators can be selected to record the biosensor amperometric signal. The careful selection of a mediator is fundamental for the successful performance of the developed device [20]. In the case of those NAD-dependent enzyme reactions, the mediator participates in the electrocatalytic regeneration of the NAD^+ cofactor. In this context, the most commonly used mediators are organics dyes [21] and inorganic redox

ions [22]. Although the mediator is commonly added in solution during the biosensor performance, a lot of work has also been done on the incorporation of the mediator on the transducer surface together with the rest of biochemicals (enzymes and cofactors) in order to construct reagentless biosensors that are easier to use and show enhanced sensitivities [23]. Selective immobilization processes are based on physically entrapment in electropolymerized layers, among others [24]. One very convenient polymer is polypyrrole (PPy) that can be easily processed in aqueous solutions at neutral pH, shows good biocompatibility, conductivity and stability.

In this work, a PPy layer was generated on the surface of a thin-film gold electrode with the aim of entrapping and thus constructing an electrochemical bienzymatic biosensor for the L-malate determination. Different redox mediators were initially tested for selecting the most suitable one in terms of signal reversibility, low oxidation potential and compatibility with the PPy membrane. A comparative study was then conducted with three different biosensor architectures based on the partial or full immobilization of the required chemical reagents in the PPy membrane. The biosensor performances were assessed in terms of working stability and analytical characteristics. The selected biosensor architecture was eventually applied to the L-malic acid monitoring during the MLF of three red wines.

2. Materials and methods

2.1. Reagents and solutions

All reagents were of high purity, analytical grade or equivalent and were purchased from Sigma-Aldrich, unless stated otherwise. All solutions were prepared using de-ionized water. For the cleaning of the electrodes, ethanol 96% and 6 M sulfuric acid (H_2SO_4) were used. Diaphorase (DP, from *Clostridium kluyveri*, lyophilized

powder, 3-20 U mg^{-1} solid) and β-Nicotinamide adenine dinucleotide hydrate (NAD^+, ≥ 96.5% enzymatic, from yeast) were stored in a freezer at -20 ºC and used as received. 15-µL 2.4 U $µL^{-1}$ Malate dehydrogenase (MDH, from porcine heart, freeze-dried material, ≥119 U mg^{-1} solid, Sorachim, S.A.) aliquots were prepared and stored in a freezer at -20 ºC. Pyrrole (reagent grade, 98%) was distilled and stored in a freezer at -20 ºC. A 0.05 M phosphate buffer solution (PB) prepared with potassium phosphate monobasic (KH_2PO_4) and adjusted at pH 7 with NaOH 0.1 M was used for all the optimization and electrochemical characterization experiments.

A set of PB solutions containing 2 mM of different compounds (2,6-Dichlorophenolindophenol sodium salt hydrate ≥ 90 %, Gallocyanine 90 %, Toluidine Blue O 80 %, Nile Blue A ≥ 75 %, 1,1′-Dimethylferrocene 95 %, Methyl Red sodium salt, Tetrathiafulvalene 97 %, Hexaammineruthenium (III) chloride ($Ru(NH_3)_6Cl_3$, 98 %) and Potassium ferricyanide ($K_3[Fe(CN)_6]$, ≥ 99 %)) were prepared for the optimization study of the redox mediator.

A set of PB solutions containing 2 mM of potassium ferricyanide, 2 mM of L-malate (L-(-)-Malic acid, Reagent Plus > 99.9%), 5 mM of NAD^+, 0.5 U DP and a different MDH activity (0 U, 1 U, 2 U, 3 U, 4 U and 5 U), were prepared for the optimization of the DP:MDH ratio. A set of PB solutions containing 2 mM of potassium ferricyanide, 2 mM of L-malate, 0.5 U DP, 3 U MDH and different NAD^+ concentrations (0 mM, 0.05 mM, 0.1 mM, 0.2 mM, 0.5 mM, 1 mM and 2 mM) were prepared for the optimization of the enzymes:co-factor ratio. For the chronoamperometric L-malate detection, a PB solution containing 0.1 M KCl, 5 mM NAD^+ and a L-malate concentration from 1×10^{-7} M to 1×10^{-5} M was used.

For the interference study, a PB solution with 0.1 M KCl, 5 mM NAD^+ and 5×10^{-7} M of the analyzed interfering compounds was prepared. The studied interferents were glycerol, glucose, gluconic acid, fructose, acetic acid, citric acid, ethanol, L-Lactate (L-(+)-lactic acid, ≥99%), tartaric acid and ascorbic acid (all them purchased from Panreac, Spain)

2.2. Devices and equipment

The thin-film gold electrodes used as transducers were fabricated on silicon substrates at the Instituto de Microelectrónica de Barcelona (IMB-CNM) according to standard microelectronic technology [25]. The chip size was 3×3.5 mm^2 and included a cell with two electrodes, namely the working electrode (WE) with an area of 1.62 mm^2 and the counter electrode (CE) with an area of 2.27 mm^2 (Fig. S1 in Supporting Information (SI)). The chips were wire-bonded on a printed-circuit board (PCB) and packaged using Ebecryl photocurable polymer following a standardized photolithographic process developed at the IMB-CNM [26].

A 20-µL poly (methyl methacrylate) (PMMA) cell was fabricated for the electrosynthesis of the polymeric membrane. Detailed information of this electrochemical cell is described in a previous work [27].

Cyclic voltammetry (CV) and chronoamperometry were performed at room temperature with an Autolab electrochemical workstation (PGSTAT-100 potentiostat – galvanostat, Ecochemie, Uthecht, The Netherlands) connected to a PC with GPES (General Purpose Electrochemical System) software. During the biosensor characterization, the three-electrode cell was completed with a Ag/AgCl (3.0 M KCl) double junction (Orion 92-02-00, Thermo Fisher Scientific Inc., Berverly, USA) reference electrode, and the integrated on-chip auxiliary electrode.

The morphological characterization of the polymeric films was carried out by scanning electron microscopy (SEM, Auriga from Carl Zeiss, Spain) and focused ion beam (FIB, Crossbeam 1560 XB from Carl Zeiss).

2.3. Optimization of the DP:MDH and (DP:MDH):NAD^+ ratios

The enzymes and co-factor relative concentrations in solution were optimized in 96-well low-binding polystyrene ELISA plates (Corning Incorporated, United States) by absorbance measurements with a Thermo Electron Multiskan EX plate reader (Thermo Fisher Scientific). Firstly, DP:MDH ratio was studied using 100-µL PB solutions containing 0.1 M KCl, 2 mM potassium ferricyanide, 2 mM L-malate and different amounts of the two enzymes. A fixed DP activity of 0.5 U was set and six activities of MDH (0 U, 1 U, 2 U, 3 U, 4 U and 5 U) were tested, these resulting in DP:MDH ratios of 1:0, 1:2, 1:4, 1:6, 1:8 and 1:10, respectively. Secondly, (DP:MDH):NAD^+ ratio was optimized using in this case 100-µL PB solutions containing 0.1 M KCl, 2 mM of potassium ferricyanide, 2 mM of L-malate, 0.5 U of DP, 3 U of MDH and different amounts of NAD^+ (0 mM, 0.05 mM, 0.1 mM, 0.2 mM, 0.5 mM, 1 mM and 2 mM) whose corresponding (DP:MDH):NAD^+ ratios were 1:0, 1:2, 1:4, 1:6, 1:8 and 1:10, respectively. Each solution was analyzed in triplicate after being stirred for 45 s and then leaving it undisturbed for 10 min for the enzymatic reaction to take place. Then, the absorbance value of the unreacted potassium ferricyanide at 405 nm wavelength was recorded [28].

2.4. Voltammetric study with different redox mediators

Following previous studies on the electrocatalytic oxidation of NADH [29, 30], eight organic compounds (2,6-Dichlorophenolindophenol sodium salt hydrate, Gallocyanine, Toluidine Blue O, Nile Blue A, 1,1′-Dimethylferrocene, Methyl Red,

Ferrocene and Tetrathiafulvalene) and two inorganic salts (Hexaammineruthenium (III) chloride (HAR) and Potassium ferricyanide) were tested as redox mediators. Cyclic voltammetric experiments were performed using the thin-film gold electrodes applied in this work, in 10 mL PB solutions (pH 7) containing 0.1 M KCl and 2 mM of each redox mediator. In the case of 1,1'-dimethylferrocene and tetrathiafulvalene, a 10% ethanol was added to the aqueous solutions in order to improve their solubility. The redox processes ascribed to each mediator were compared in terms of reversibility, current and redox potential values as well as solubility. Ideally, a mediator showing a fully reversible redox process taking place at low potentials, in order to avoid interferences from other species that may be present in the wine samples, and showing a high current density is pursued. Also, these species should have good water solubility to allow for the strict control of the polypyrrole membrane electrosynthesis.

The redox mediators that best meet all these characteristics were incorporated into a PPy membrane generated on the transducer surface, as described below.

2.5. Electrosynthesis of the polymeric membranes

Before the electrogeneration of the PPy layer, the thin-film gold electrodes were cleaned and activated [25]. The conditions for the electrosynthesis on the surface of the gold transducers were optimized elsewhere [27]. Using the PMMA cell mentioned above and a Ag wire as pseudo-reference electrode, a +0.85 V potential was applied in a PB solution containing 0.4 M pyrrole (monomer) and 0.1 M KCl (counter-ion). The PPy membrane was electrosynthesized in two consecutive potentiostatic steps. In the first step, the redox mediator was entrapped in a PPy membrane for ensuring the good electron transfer with the transducer surface and avoiding competition with the other species (enzymes and cofactor) during the membrane growth. The concentration of the

redox mediator was fixed to 10 mM for ensuring its excess against the other chemical reagents involved in the bienzymatic process. The accumulation charge during this electrosynthesis was fixed to 250 mC cm^{-2}. In the second step, the enzymes (MDH and DP) and the cofactor (NAD^+) were entrapped in a new PPy membrane, fixing the accumulation charge to 500 mC cm^{-2}. This accumulation charge enabled the efficient entrapment of enzymes as has been previously demonstrated by our group [27]. Current profiles recorded during the potentiostatic generation of the PPy/redox mediator and the PPy/enzyme films are depicted in Fig. S2 (in the SI).

Using these electrosynthesis conditions, three different biosensor architectures that differ in the immobilization of the different components, were assessed: Biosensor 1, the mediator was not immobilized and the sensor performance was tested in solutions containing the selected mediator; Biosensor 2, the NAD^+ cofactor was not immobilized and the sensor performance was tested in solutions containing this cofactor and Biosensor 3, both the redox mediator and the cofactor were immobilized on the electrode surface.

2.6. Chronoamperometric measurements

Chronoamperometric measurements were carried out by applying a set overpotential that depended on the selected redox mediator. This potential allows re-oxidizing the reduced mediator generated during the bienzymatic process and the faradaic current recorded is stoichiometrically related to the L-malate concentration in the sample (see more details in Fig S3 in SI). The biosensors were calibrated in 10 mL PB solutions (pH 7) containing L-malate in a concentration range between 1×10^{-7} M and 1×10^{-5} M. All the measurements were done by triplicate.

Firstly, a study on the working stability of the different biosensor architectures was performed. The study consisted of periodic calibrations for over 40 days. The biosensors were stored in PB at 4 ºC when not in use.

Once the more stable architecture was selected, the biosensor performance was assessed in terms of repeatability, reproducibility, sensitivity, linear range and limit of detection to L-malate using three biosensors fabricated under the same experimental conditions.

In order to evaluate the selectivity of the optimized biosensor, chronoamperometric measurements were performed in PB solutions containing 5×10^{-7} M concentrations of glycerol, glucose, gluconic acid, fructose, acetic acid, citric acid, ethanol, L-lactate, tartaric acid, or ascorbic acid as interferences.

2.7. Analysis of real samples coming from wine malolactic fermentation processes

A study with wine samples was conducted in order to evaluate the applicability of the developed bienzymatic biosensor. Three red wines (2013 vintage, from Tarragona, Spain) based on Marcelanne, Petit Verdot and Syrah grape varieties, were provided by the Catalan Institute of Vineyard and Wine (IRTA-INCAVI). In these wines, the malolactic fermentation was induced by inoculation of a strain of *Oenococcus oeni* lactic acid bacteria. The analyzed samples were collected periodically during the malolactic fermentation process. They had a concentration of L-malic acid from 0 to 2×10^{-2} M (0 – 2.5 g L^{-1}). Ten samples from the Marcelanne wine (“Wine 1”) along 32 days, 5 samples from the Petit Verdot wine (“Wine 2”) along 15 days and 11 samples from the Syrah wine (“Wine 3”) along 34 days were analyzed with the developed biosensor. These samples were diluted 1:20000 (“Wine 1"), 1:25000 (“Wine 2”) and 1:10000 (“Wine 3”) in PB solution to adjust the L-malic acid concentration to

the linear range of the amperometric biosensor. The high sensitivity of the biosensor allowed these high dilutions of the wine samples, thus avoiding the potential matrix effects that could interfere in the determination. The results obtained were compared with the standard enzymatic method used by the IRTA-INCAVI. This is an enzymatic catalyzed reaction between the L-malate and the NAD^+ to produce NADH, whose concentration increase is measured by absorbance at 340 nm and stoichiometrically related to the L-malate concentration in the samples [10].

3. Results and discussion

3.1. Selection of the DP:MDH and (DP:MDH):NAD^+ ratios

The enzymes and cofactor relative concentrations were optimized and results are shown in Fig. 1. The absorbance value decreased with the increase of MDH activity up to 3 U, remaining constant for higher values. Thus, the optimum DP:MDH ratio was 1:6. Then, the DP and MDH activities were fixed to 0.5 U and 3 U, respectively, and the NAD^+ concentration was increased from 0 to 2 mM. The recorded absorbance values levelled off for NAD^+ concentrations above 0.5 mM. Thus, the (DP:MDH):NAD^+ ratio was set to 2:1. These ratios were selected for the further biosensor fabrication.

3.2. Selection of the redox mediator

All the selected redox mediators of this study have previously been applied in amperometric biosensing [29, 30]. The corresponding cyclic voltammograms recorded with the thin-film gold electrodes are shown in Fig. S4 and Fig. S5 in SI. Unlike in those reported studies that make use of these mediators, the expected quasi-reversible signals could not be recorded with all of them. This might be related to the use of a gold electrochemical transducer instead of the carbon-based transducers applied in those works. Table 1 includes the electrochemical parameters extracted from these

voltammograms. Using the oxidation potential (E_{ox}) as the initial parameter to select these species, the lowest values were obtained for Gallocyanine, Toluidine Blue O and HAR (-250 mV, -275 mV and -180 mV, respectively). Among these three redox mediators, Gallocyanine and Toluidine Blue O showed a similar peak potential separation (ΔE_p), while this is about two times larger for HAR. Then, the ratio of oxidation to reduction peak currents was compared. Values around 1 indicate the absence of coupled chemical reactions. This is the case for Gallocyanine and HAR, while is around 2.1 for Toluidine Blue O. These three redox mediators showed oxidation peak current densities higher than 250 µA cm^{-2}. Besides, all three are fully water soluble, therefore the electrosynthesis conditions of the PPy would not be modified by presence of any organic solvent.

Then, the electrogeneration of the PPy/mediator membrane on the surface of the gold transducers was carried out in solutions containing 10 mM of each of these three redox mediators. Toluidine Blue O formed a blue precipitate during the polymerization process. This is likely to be related to the polymerization of this redox mediator by the one-electron oxidation of the NH_2 group and the formation of a radical cation at the potential applied during the PPy electrosynthesis membrane [31]. By contrast, both Gallocynine and HAR could be entrapped in the PPy membrane and the time to achieve an accumulation charge of 250 mC cm^{-2} was 70 and 30 s, respectively. The resulting membranes were rinsed with PB and tested by cyclic voltammetry and then stored immersed in PB solution at 4 ºC. After 24 h, the PPy/Gallocyanine- modified transducer nearly lost all its voltammetric response and the PB solution turned blue-colored, meaning that the mediator leached from the polypyrrole membrane. This may be due to charge repulsion between the positively charged pyrrole and the Gallocyanine molecules during the PPy membrane electrosynthesis that would make these species not

to be efficiently entrapped and thus to be easily leached. The same experiment was repeated with PPy/HAR-modified transducer, this keeping its voltammetric response after the 24-h period. Therefore, this redox mediator was selected for the fabrication of the biosensor architecture.

3.3. Selection of the biosensor architecture

The working stability of the three different biosensor architectures, described in section 2.5, was analyzed for over 40 days. The lifetime estimated from the percentage of the initial sensitivity kept over time, is shown in Fig. 2. In the three cases, an initial decrease of the sensitivity is observed during the first eight days, probably related to partial leaching of the chemical species not tightly immobilized within the PPy membrane. This decrease was more pronounced for biosensor 3 (all reagents in the PPy membrane), which lost 30% sensitivity after 5 days and 45 % after 8 days, and biosensor 1 (redox mediator in solution), which lost 10 % sensitivity after 3 days, 20% after 7 days and 40% after 18 days. However, biosensor 2 architecture (NAD^+ in solution) just lost 10 % after 37 days. The decrease in sensitivity of biosensor 1 and 3 is likely to be due to the fast decomposition of the entrapped NAD^+ [32]. Biosensor 2 appeared to be the most suitable for the monitoring of L-malic acid during the red wine fermentation process, taking into account that it maintained around 90% of the initial sensitivity after 37 days. Then it suddenly decreased to 30 % of the initial value after 42 days, probably due to the denaturation of the immobilized enzymes. This architecture was then selected and fully characterized, as described in the following sections.

3.4. Morphological characterization of the PPy films

The thickness and morphology of the electrogenerated PPy membranes are influenced by some experimental parameters, such as applied potential and accumulated

charge during the electrosynthesis, counter-ion required for the PPy polymerization, as well as the chemical and biochemical species entrapped in the resulting membrane and present in the polymerization solution [33]. The PPy membrane thicknesses, measured by FIB, (Fig. S6 in SI) was 1.3 µm and 2.5 µm for the PPy/HAR and the PPy/(DP:MDH) membranes, respectively. This difference is in accordance with the electrical charge associated to the electrosynthesis of both membranes, being twice for the PPy/(DP:MDH) membrane than that of the PPy/HAR one. An additional SEM image (Fig. S6 in SI) showed the homogeneity and roughness of the PPy membranes.

3.5. Evaluation of the biosensor performance

The optimized biosensor was calibrated by chronoamperometry in PB solutions containing 0.1 M KCl, 5 mM NAD^+ and a L-malate concentration ranging from 1×10^{-7} M to 1×10^{-5} M. A -0.15 V potential (vs. Ag/AgCl) was chosen considering the voltammetric response of the selected redox mediator (Fig. S5 de la SI), at which the HAR reduced species generated by the enzymatic reaction are oxidized back to the HAR. Results are shown in Fig. 3 A. The sensor response followed an exponential trend, and the current started to level off at 70 s time after initiating the measurement. The signal was recorded during 120 s and the mean current density value of the last 20 s was used as analytical signal. As expected, the recorded current density increased with the L-malate concentration. Then, it can be said that the biosensor response was 70 s and the overall assay time is set to 120 s. The calibration curve is shown in Fig. 3 B. A linear range was observed in a concentration range from 1×10^{-7} M – 1×10^{-6} M (1.3×10^{-5} – 1.3×10^{-4} g L^{-1}) of L-malate with a sensitivity of 1365±110 mA M^{-1} cm^{-2} (r = 0.998, n = 5). A limit of detection of 6.3×10^{-8} M, calculated using the 3σ IUPAC criterion, was obtained. For L-malate concentration above 1×10^{-6} M, the biosensor response is

saturated, this following the usual behavior of a Michaelis-Menten kinetic process. Regarding the biosensor reproducibility, three different devices were calibrated on the same day, obtaining a relative standard deviation (RSD) of the sensitivity lower than 10 %.

The biosensor selectivity to L-malate was assessed considering the possible interferences found in wine. Results are shown in Fig. 4. Among all of them, just ascorbic acid produced a non-negligible biosensor response that is related to the irreversible electrochemical oxidation that starts at the applied potential of -0.15 V and whose maximum anodic peak current appears at -0.066 V [34]. Although ascorbic acid exists in small quantities in grapes (around 10 mg L^{-1} or 7.5×10^{-5} M), it rapidly disappears during the fermentation and initial aeration processes [3]. Therefore, it is anticipated that the red wine samples coming from the malolactic fermentation process would not contain ascorbic acid. Therefore, it can be stated that the L-malate determination is not affected by the presence of interferences.

3.6. Application of the biosensor in real wines samples from malolactic fermentation

The biosensor performance for the L-malate determination in wine samples collected during the malolactic fermentation was assessed. Fig. 5 shows the results of the analysis of samples collected from the fermentation process of three red wines and the values obtained with the standard colorimetric method. An excellent agreement was achieved with absolute errors below 0.2 g L^{-1} (1.5×10^{-3} M) in all the samples. As can be seen, almost all values obtained with the biosensor are within the uncertainty range at 95% of the standard method. The evolution of the malic acid during the fermentation processes was as expected. When the concentration of L-malic is below 0.3 g L^{-1} (2.2×10^{-3} M) for 3 consecutive determinations, the transformation to L-lactic acid

ended. In this case, the three wines analyzed have completed this process. During the winemaking, the detection of this end point is very important in order to microbiologically stabilize the wine by adding sulphite on time. If not, the lactic acid bacteria begin to degrade the sugars, producing an increase of acetic acid concentration in wine. This affects negatively the taste and odor of the final product. It is worth mentioning that all measurements performed in this study were carried out with the same biosensor, which retained the 90% of its initial sensitivity after analyzing more than 80 measurements, including all the wine samples as well as the calibrations carried out before and after the analysis of each wine.

3.7. Comparative study with other L-malate amperometric biosensors

Table 2 shows the analytical characteristics of the developed L-malate biosensor and other amperometric biosensors based on the use of MDH, previously reported. Regarding the application of coupled enzyme reactions, there is one biosensor using just MDH and most of them also incorporate DP for improving the sensitivity. The biosensor described in this work clearly outperforms the other approaches in terms of sensitivity and detection limit. This may be partially related with the immobilization of the chemical species in a conductive polypyrrole membrane synthesized under biocompatible conditions that may preserve the enzyme activity almost intact. Besides, using an electropolymerization approach such as the one described in this work enables the strict controlled deposition of the required chemical species making it compatible with the application of miniaturized transducers. By contrast, the estimated biosensor linear range is slightly shorter than that shown by other devices. It is suggested that this may be related to the limited amount of mediator entrapped in the polymer film compared with that when the mediator is kept in solution. Nevertheless, immobilizing

the mediator together with the enzymes is highly desirable in order to minimize the number of reagents added to the measuring solution.

A biosensor applied to the monitoring of the malolactic fermentation must show a long-term working stability under continuous use because the fermentation process takes around 30 days. Some of the biosensors in Table 2 show storage stability values, showing excellent results after months or years. However, the working biosensor stability is significantly worse, this being restricted to few days and thus limiting the biosensor performance for the proposed application. The biosensor developed in this work maintains 90 % of its initial sensitivity after 37 days in solution and continuous use, being the only amperometric biosensor based on MDH reported so far that could be applied to the real-time monitoring of malolactic fermentation processes. Finally, some biosensors have been applied to the determination of L-malate in wines samples and one of them has been tested in synthetic wines samples simulating the malolactic fermentation process. However, the biosensor presented in this work is the only one that has been assessed using real samples collected during the malolactic fermentation of red wines.

4. Conclusions

An electrochemical bienzymatic biosensor for the determination of L-malate based on the co-entrapment of MDH and DP enzymes together with the redox mediator in an electrosynthesized PPy film has been developed. The study performed with 10 different redox mediators demonstrated that the Hexaammineruthenium (III) chloride can be effectively entrapped in the PPy film. Although the incorporation of the NAD^+ as enzymatic cofactor into the PPy membrane was also assessed, the working stability was limited by the chemical decomposition of NAD^+. The results demonstrated that the

developed biosensor presented a very high sensitivity with a low limit of detection. Besides, the biosensor retained more than 90 % of its original sensitivity over 37 days of performance, allowing its successful application to the L-malic acid monitoring during the malolactic fermentation of three red wines.

Acknowledgements

We acknowledge funding from the Spanish R & D National Program (MINECO, Project TEC2011-29045-C04-01 and 04). P. G.-G. is grateful to MINECO, Spain, for the financial support through a research studentship of the FPI Program. We also acknowledge the group of Dr. Iluminada Gallardo (Chemistry Department, Universitat Autònoma de Barcelona, Spain) for the support during the polymer distillation.

Appendix A. Supplementary data

Supplementary data related to this article can be found in the online version.

References

1. Ford, C.M., The Biochemistry of Organic Acids in the Grape, in The Biochemistry of the Grape Berry, H. Gerós, M. Chaves, and S. Delrot, Editors. 2012, Bentham Books. p. 67-88.

2. Boulton, R.B., et al., Principles and Practices of Winemaking. 1999, New York: Springer Science + Business Media.

3. Ribereau-Gayon, P., et al., Handbook of Enology. 2 ed. Vol. 1, The Microbiology of Wine and Vinifications. 2006: John Wiley & Sons Ltd,.

4. Bony, M., et al., Metabolic analysis of S-cerevisiae strains engineered for malolactic fermentation. Febs Letters, 1997. 410(2-3): p. 452-456.

5. Calull, M., R.M. Marce, and F. Borrull, Determination of carboxylic-acids, sugars, glycerol and ethanol in wine and grape must by ion-exchange high-performance liquid-chromatography with refractive-index detection. Journal of Chromatography, 1992. 590(2): p. 215-222.

6. Kelebek, H., et al., HPLC determination of organic acids, sugars, phenolic compositions and antioxidant capacity of orange juice and orange wine made from a Turkish cv. Kozan. Microchemical Journal, 2009. 91(2): p. 187-192.

7. Vonach, R., B. Lendl, and R. Kellner, High-performance liquid chromatography with real-time Fourier-transform infrared detection for the determination of carbohydrates, alcohols and organic acids in wines. Journal of Chromatography A, 1998. 824(2): p. 159-167.

8. Esteves, V.I., et al., Using capillary electrophoresis for the determination of organic acids in Port wine. Analytica Chimica Acta, 2004. 513(1): p. 163-167.

9. Mato, I., S. Suarez-Luque, and J.F. Huidobro, Simple determination of main organic acids in grape juice and wine by using capillary zone electrophoresis with direct UV detection. Food Chemistry, 2007. 102(1): p. 104-112.

10. L-malic acid: enzymatic method (OIV Compendium ed. 1990, revised by 377/2009) , OIV-MA-AS313-11 2009, International Organisation of Vine and Wine (OIV).

11. Bucur, B., et al., Strategies to develop malic acid biosensors based on malate quinone oxidoreductase (MQO). Biosensors & Bioelectronics, 2006. 21(12): p. 2290-2297.

12. Esti, M., et al., Electrochemical biosensors for monitoring malolactic fermentation in red wine using two strains of Oenococcus oeni. Analytica Chimica Acta, 2004. 513(1): p. 357-364.

13. Gurban, A.M., et al., Malate biosensors for the monitoring of malolactic fermentation: Different approaches. Analytical Letters, 2006. 39(8): p. 1543-1558.

14. Mazzei, F., F. Botre, and G. Favero, Peroxidase based biosensors for the selective determination of D,L-lactic acid and L-malic acid in wines. Microchemical Journal, 2007. 87(1): p. 81-86.

15. Gallarta, F., F. Javier Sainz, and C. Saenz, Fluorescent sensing layer for the determination of L-malic acid in wine. Analytical and Bioanalytical Chemistry, 2007. 387(6): p. 2297-2305.

16. de Santana, J.F.S., M.F. Belian, and A.F. Lavorante, A Spectrophotometric Procedure for Malic Acid Determination in Wines Employing a Multicommutation Approach. Analytical Sciences, 2014. 30(6): p. 657-661.

17. Gamella, M., et al., Integrated multienzyme electrochemical biosensors for monitoring malolactic fermentation in wines. Talanta, 2010. 81(3): p. 925-933.

18. Monosik, R., et al., Comparison of biosensors based on gold and nanocomposite electrodes for monitoring of malic acid in wine. Central European Journal of Chemistry, 2012. 10(1): p. 157-164.

19. Grieshaber, D., et al., Electrochemical biosensors - Sensor principles and architectures. Sensors, 2008. 8(3): p. 1400-1458.

20. Chaubey, A. and B.D. Malhotra, Mediated biosensors. Biosensors & Bioelectronics, 2002. 17(6-7): p. 441-456.

21. Schlereth, D.D., E. Katz, and H.L. Schmidt, Surface-modified gold electrodes for electrocatalytic oxidation of NADH based on the immobilization of phenoxazine and phenothiazine-derivatives on self-assembled monolayers. Electroanalysis, 1995. 7(1): p. 46-54.

22. Somasundrum, M., J. Hall, and J.V. Bannister, Amperometric NADH determination via both direct and mediated electron-transfer by NADH oxidase from thermus-aquaticus YT-1. Analytica Chimica Acta, 1994. 295(1-2): p. 47-57.

23. Barendrecht, E., Chemically and physically modified electrodes- Some new developments. Journal of Applied Electrochemistry, 1990. 20(2): p. 175-185.

24. Teles, F.R.R. and L.R. Fonseca, Applications of polymers for biomolecule immobilization in electrochemical biosensors. Materials Science & Engineering C-Biomimetic and Supramolecular Systems, 2008. 28(8): p. 1530-1543.

25. Orozco, J., et al., Characterization of ultramicroelectrode arrays combining electrochemical techniques and optical microscopy imaging. Electrochimica Acta, 2007. 53(2): p. 729-736.

26. Jimenez-Jorquera, C., J. Orozco, and A. Baldi, ISFET Based Microsensors for Environmental Monitoring. Sensors, 2010. 10(1): p. 61-83.

27. Gimenez-Gomez, P., et al., Monitoring of malolactic fermentation in wine using an electrochemical bienzymatic biosensor for L-lactate with long term stability. Analytica Chimica Acta, 2016. 905: p. 126-133.

28. Chakrabarti, M.H. and E.P.L. Roberts, Analysis of Mixtures of Ferrocyanide and Ferricyanide using UV-Visible Spectroscopy for Characterisation of a Novel Redox Flow Battery. Journal of the Chemical Society of Pakistan, 2008. 30(6): p. 817-823.

29. Gründig, B. et al., Mediator-modified electrodes for electrocatalytic oxidation of NADH. Journal of Electroanalytical Chemistry, 1995. 395: p. 143-157.

30. Schuhmann, W. et al., Electrocatalytic oxidation of NADH at mediator-modified electrodes surfaces. Journal of Biotechnology, 1993. 27: p. 129-142.

31. Zeng, J., et al., Fabrication of poly(toluidine blue O)/carbon nanotube composite nanowires and its stable low-potential detection of NADH. Journal of Electroanalytical Chemistry, 2006. 595(2): p. 152-160.

32. Nicotinamide cofactor dependent oxidoreductions, in Enzymes synthetic organic chemistry, C.H. Wong and G.M. Whitesides, Editors. 1994, Pergamon. p. 131-153.

33. Curtin, L.S., G.C. Komplin, and W.J. Pietro, Diffusive anion-exchange in polypyrrole films. Journal of Physical Chemistry, 1988. 92(1): p. 12-13.

34. Borsook, H. and G. Keighley, Oxidation reduction potential of ascorbic acid (Vitamin C). Proceedings of the National Academy of Sciences of the United States of America, 1933. 19: p. 875-878.

35. Miertus, S., et al., Amperometric biosensors based on solid binding matrices applied in food quality monitoring. Biosensors & Bioelectronics, 1998. 13(7-8): p. 911-923.

36. Katrlik, J., et al., Biosensors for L-malate and L-lactate based on solid binding matrix. Analytica Chimica Acta, 1999. 379(1-2): p. 193-200.

37. Arvinte, A., L. Rotariu, and C. Bala, Amperometric low-potential detection of malic acid using single-wall carbon nanotubes based electrodes. Sensors, 2008. 8(3): p. 1497-1507.

Table 1.Chemical structures of the studied redox mediators and their main redox values obtained in solution: oxidation potential (E_{ox}), peak potential separation (ΔE_p) and the ratio between the oxidation and the reduction peak currents (I_{ox}/I_{red})

Redox mediator	Chemical structure	E_{ox} / mV	ΔE_p/ mV	$\lvert I_{ox}/I_{red} \rvert$
2,6-Dichlorophenolindophenol sodium salt hydrate	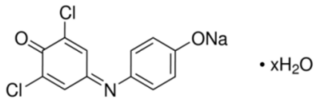	10	55	0.4
Gallocyanine	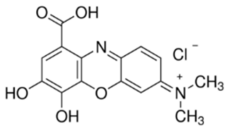	-250	59	0.9
Toluidine Blue O	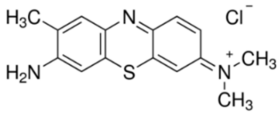	-274	66	2.1
Nile Blue A*	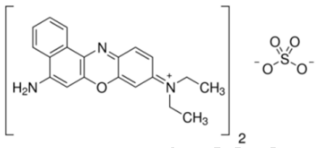	-	-	-
1,1′-Dimethylferrocene	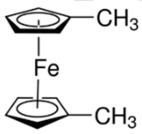	68	57	1.7
Methyl Red	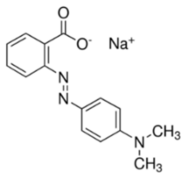	126	205	0.9
Ferrocene	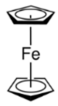	190	85	1.3
Tetrathiafulvalene	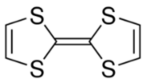	110	94	1.8
Hexaammineruthenium (III) chloride	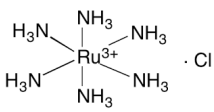	-180	80	0.9
Potassium ferricyanide(III)	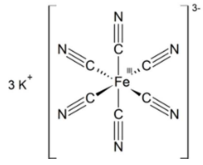	220	120	0.8

**There is no signal of the oxidation peak current*

475 **Table 2.** L-malate amperometric biosensors based on MDH described in the literature.

Enzymes	Electrode	Mediator	Immobilization	Sensitivity ($\mu A\ M^{-1}$)	Linear range (M)	LOD (M)	Stability	Samples	Reference
MDH/DP	Carbon-Paste	Ferricyanide in solution	entrapment in the carbon paste	-	1.5×10^{-5} - 1.5×10^{-3}	1.5×10^{-5}	90 % after 1 month of storage	-	[35]
MDH/DP	Carbon	Ferricyanide in solution	dialysis membrane	-	1×10^{-5} – 1.3×10^{-3}	1×10^{-5}	100 % after 5 month of storage or 5 assays	Wines	[36]
MDH	SWCNT		physical absorption	4.55×10^{-1}	2×10^{-4} - 8×10^{-4}	$3.3.\times10^{-7}$	75 % after 5 measures	-	[37]
MDH/DP	Gold planar electrode	Ferricyanide in solution	chitosan layers	5.50×10^{-4}	1.5×10^{-6} - 5.2×10^{-4}	5.4×10^{-6}	63 % after 7 days or 30 assays or 90 % after 1 year of storage	Wines	[18]
MDH/DP	Gold disk	TTF	MPA-SAM and dialysis membrane	1.58×10^{3}	5.2×10^{-7} - 2×10^{-5}	5.2×10^{-7}	90 % after 7 days	Synthetic MLF	[17]
MDH/DP	Thin-film gold electrode	Hexaammine ruthenium (III) chloride	PPy entrapment	2.18×10^{4}	1×10^{-7} - 1×10^{-6}	6.3×10^{-8}	90 % after 32 days or 80 assays	Red wines from MLF	This work

476 *TTF: tetrathiafulvalene; MPA: 3-mercaptopropinic acid; SAM: self-assembled monolayer; SWCNT: single-wall carbon nanotubes;*

Figure Captions

Fig. 1. Absorbance recording of ferricyanide for different biocomponents ratios a) DP:MDH and b) (DP:MDH):NAD^+. Measurements were carried out in PB solution containing 2 mM potassium ferriyanide, 2 mM L-malate and different concentration of DP, MDH and NAD^+. Each point corresponds to the mean value of three replicates and the error bars represents the standard deviation.

Fig. 2. Comparative study of the working stability along 38 days for the three proposed biosensor architectures: biosensor 1 (green colored stars), biosensor 2 (red colored triangles), and biosensor 3 (blue colored circles),

Fig. 3 A) Chronoamperometric response of the developed biosensor for L-malate concentrations in a range of 1×10^{-7} M (a) to 5×10^{-6} M (g). B) Calibration curve for L-malate representing the mean current value of three replicates recorded consecutively with the same biosensor. The error bars correspond to the standard deviation.

Fig. 4. Current density response of the biosensor in solutions containing different interferents at a concentration of 5×10^{-7} M.

Fig. 5. Comparative analysis of wine samples collected during the malolactic fermentation process for three red wines. Dashed lines and circles show the values of L-malic acid measured with the developed biosensor and solid lines and squares, those obtained with the colorimetric standard method. The error bars represent the uncertainty at 95 % in the case of the colorimetric method.

Fig. 1

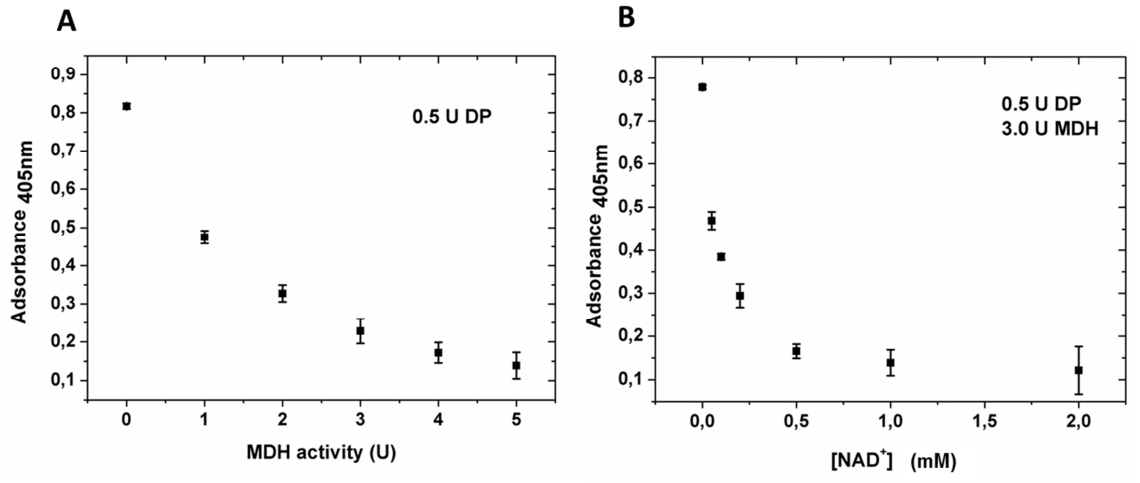

Fig. 2

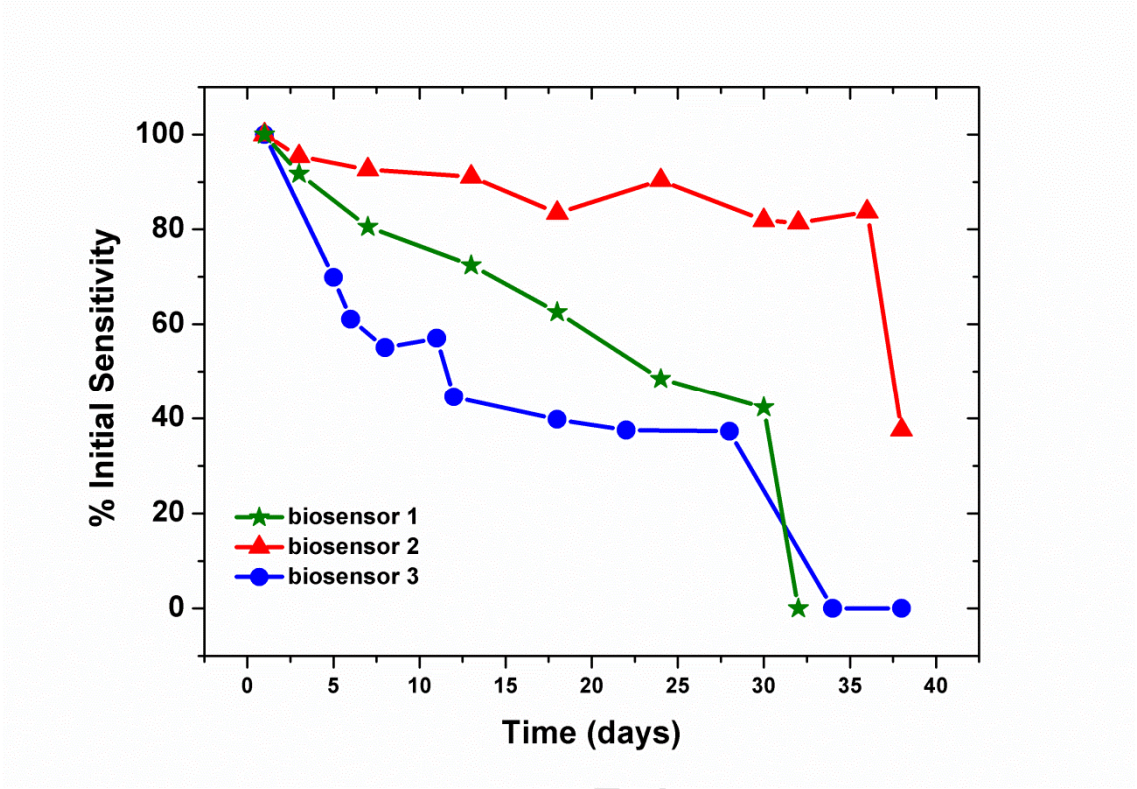

Fig. 3

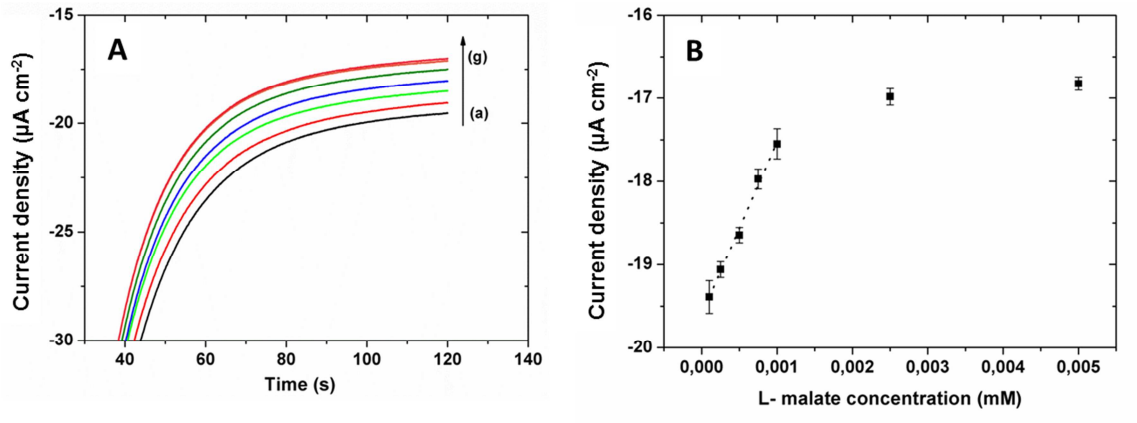

Fig. 4

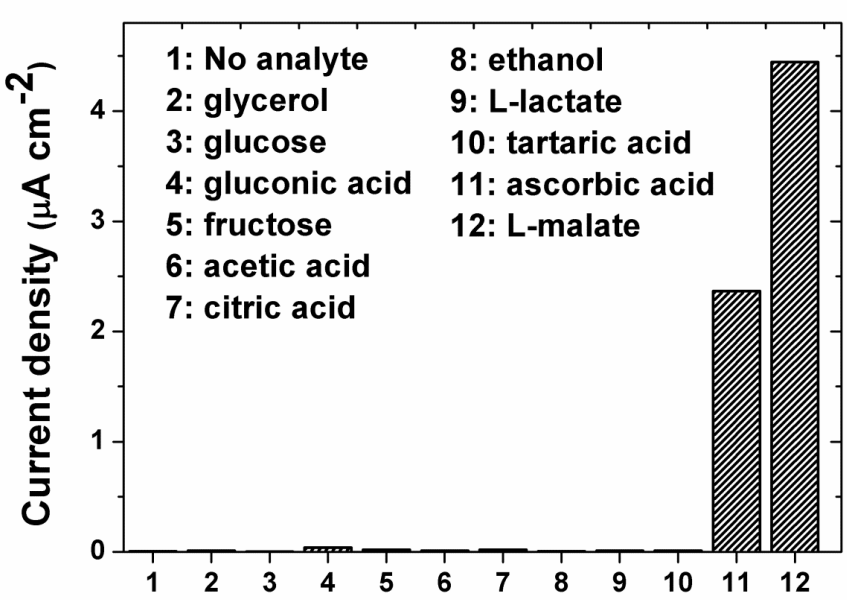

Fig. 5

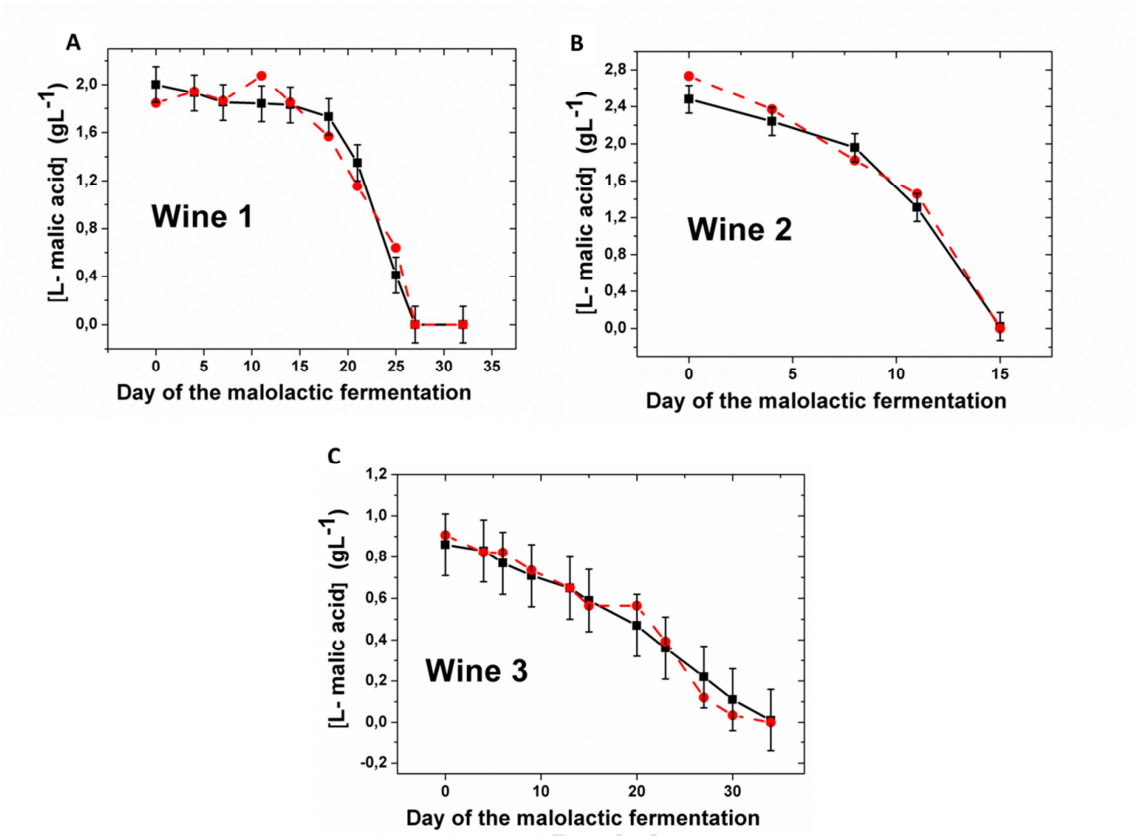

497

HIGHLIGHTS

- Bienzymatic electrochemical biosensor for L-malate.
- Malate dehydrogenase and diaphorase enzymes entrapped into a electrosynthesized polypyrrole film.
- Optimized redox mediator also incorporated into the polymeric film.
- Long-term stability for over 37 days.
- Application to L-malic acid determination during the malolactic fermentation of red wines.

ROBUST L-MALATE BIENZYMATIC BIOSENSOR TO ENABLE THE ON-SITE MONITORING OF MALOLACTIC FERMENTATION OF RED WINES

Pablo Giménez-Gómez[a], Manuel Gutiérrez-Capitán[a*], Fina Capdevila[b], Anna Puig-Pujol[b], Cesar Fernández-Sánchez[a] and Cecilia Jiménez-Jorquera[a]

[a] *Instituto de Microelectrónica de Barcelona (IMB-CNM), CSIC, Campus UAB, 08193 Bellaterra, Spain*

[b] *Institut Català de la Vinya i el Vi (IRTA-INCAVI), Plaça Àgora 2, 08720 Vilafranca del Penedès, Spain*

[*] *Corresponding author:* Manuel Gutiérrez-Capitán, *email:* manuel.gutierrez@csic.es

Supporting Information

INDEX OF SUPPLEMENTARY FIGURES

a)

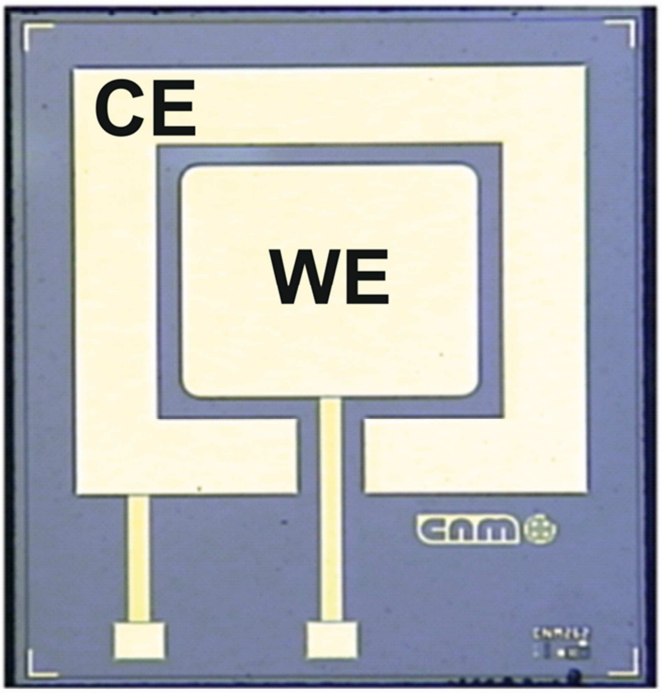

b)

Fig. S1. A) Picture of the silicon chip with a two-electrode cell. B) Picture showing the relative size of the chip.

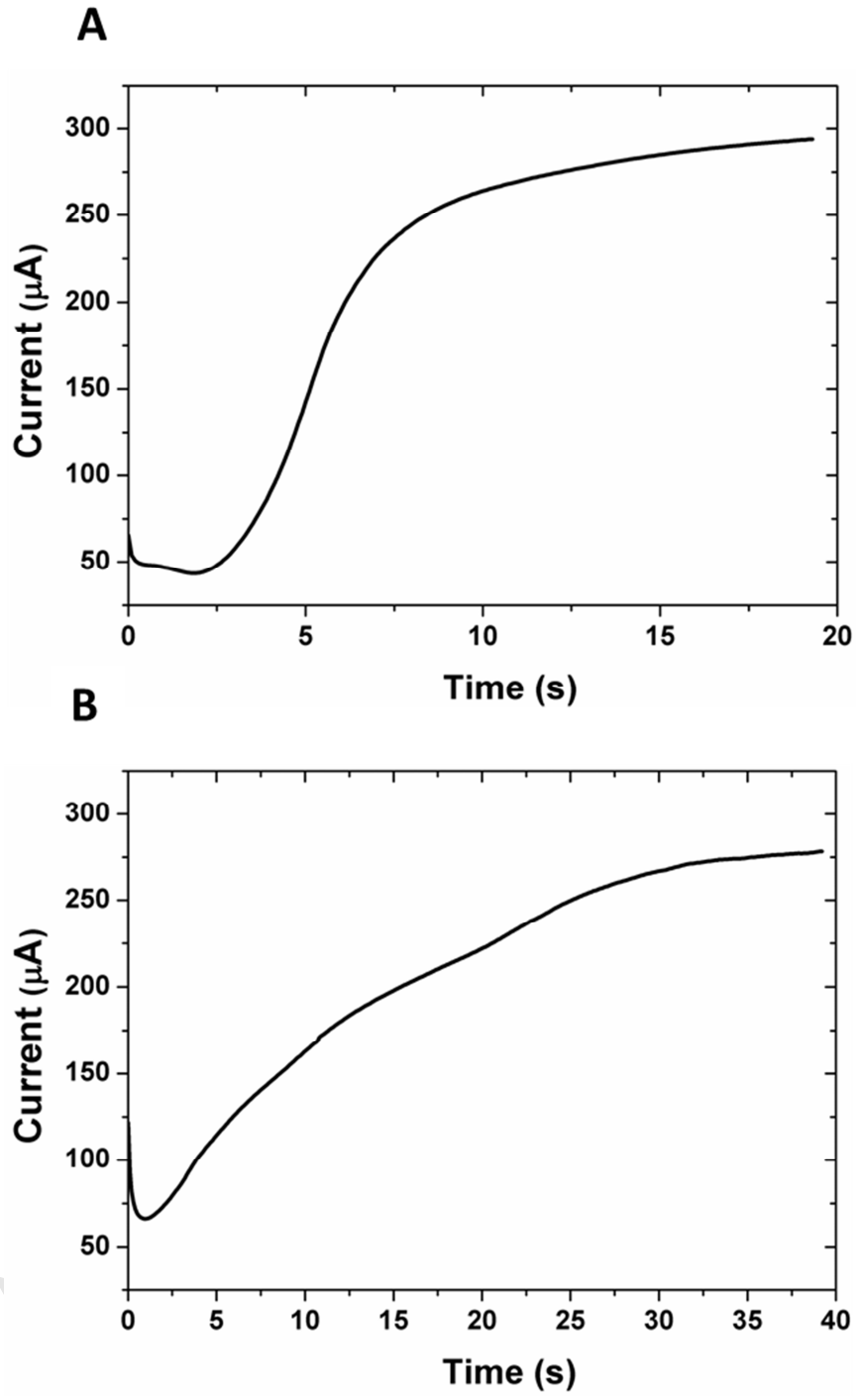

Fig. S2. Current profile recorded during the potentiostatic generation of the (A) PPy/redox mediator film and the (B) PPy/enzyme film.

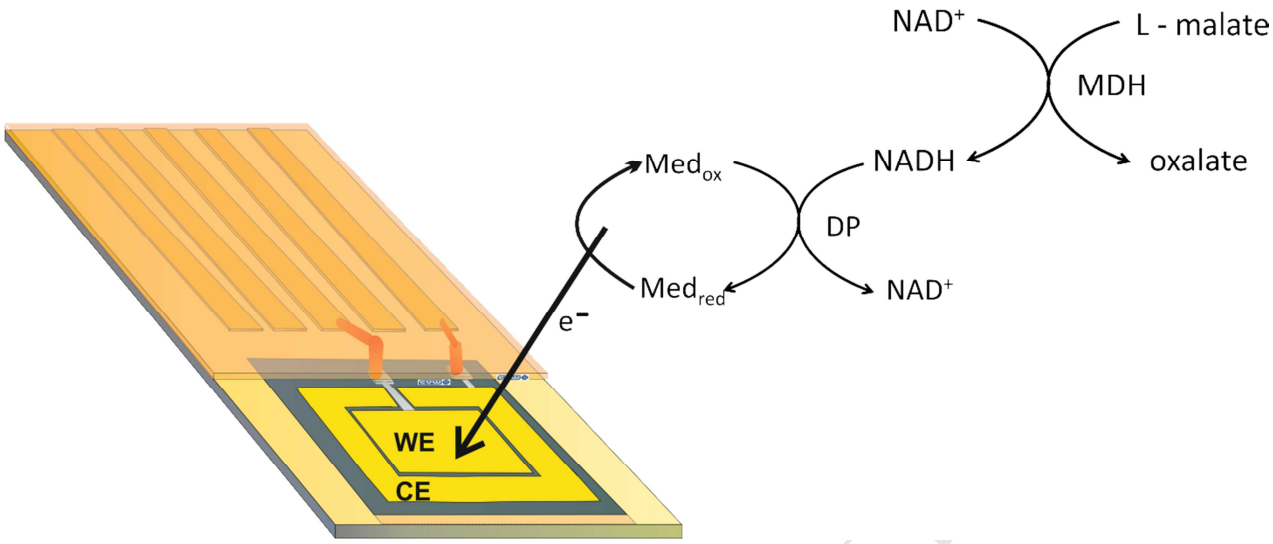

Fig. S3. Scheme of the bi-enzymatic reactions associated to the L-malate detection.

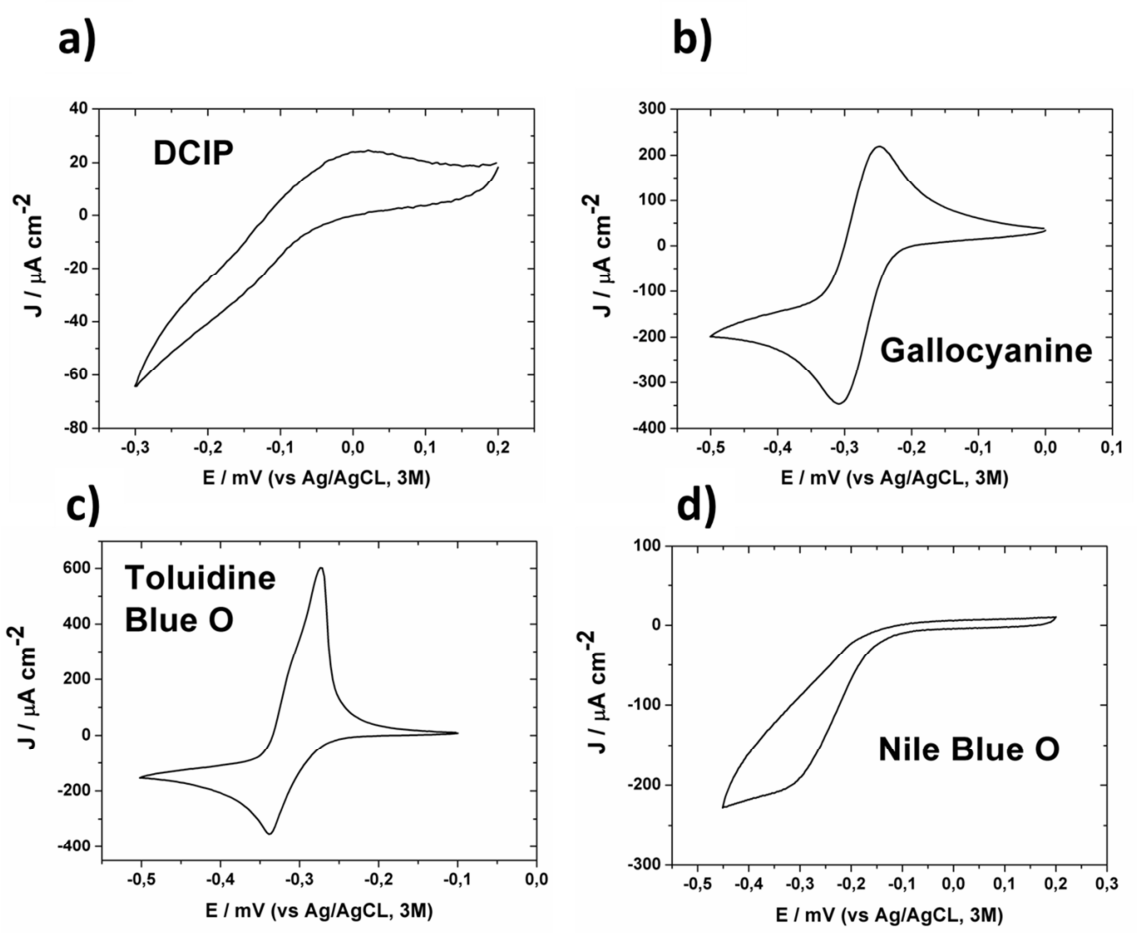

Fig. S4. Cyclic voltammograms recorded in PBS buffer containing 2 mM of the mediator: a) 2,6-dichlorophenolindophenol sodium salt hydrate; b) Gallocyanine;, c) Toluidine Blue O and d) Nile Blue A . Scan rate = 25 mV s^{-1}

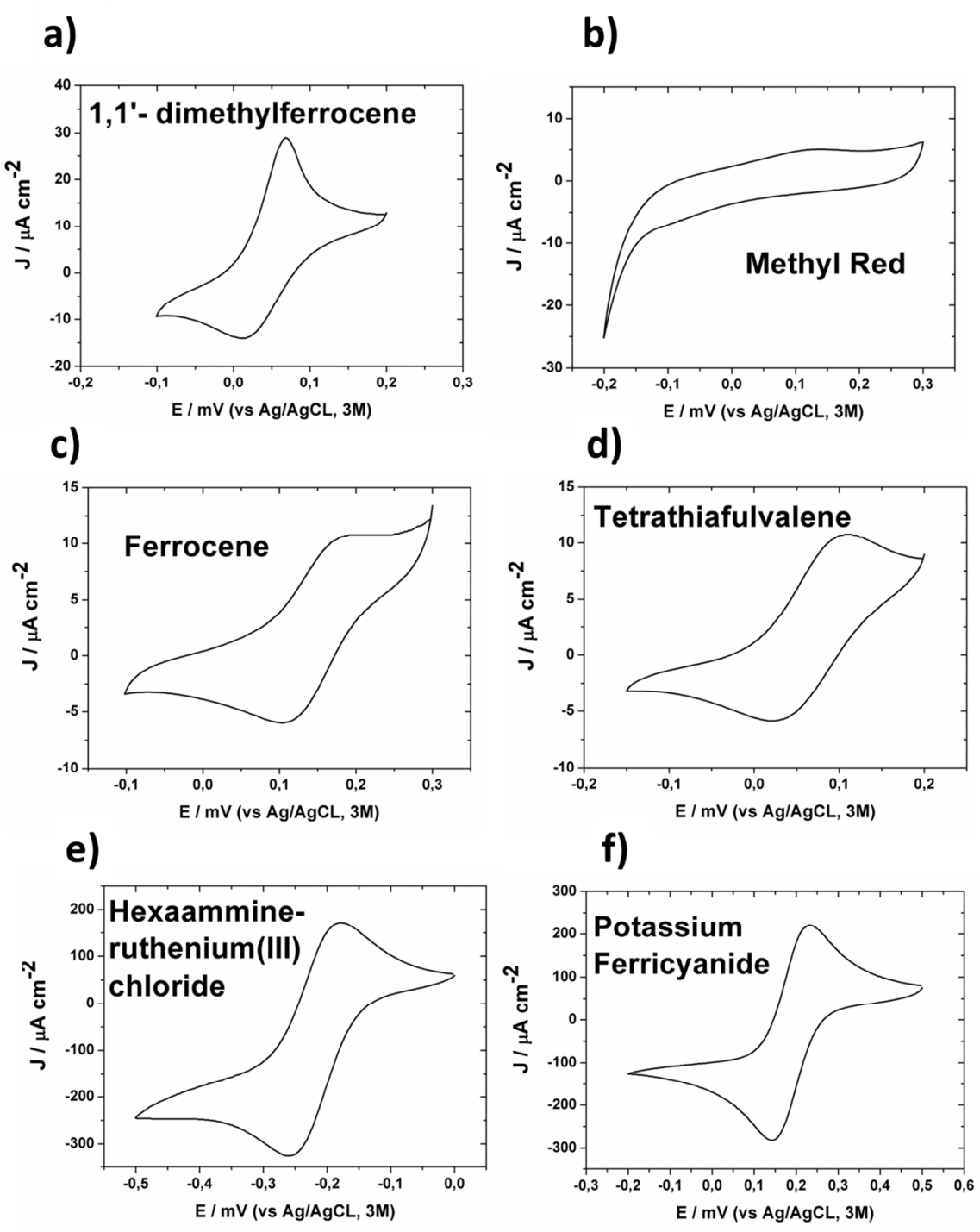

Fig. S5. Cyclic voltammograms recorded in PBS buffer containing 2 mM of the mediator: a) 1,1-dimethylferrocene; b) Methyl Red; c) Ferrocene; d) Tetrathiafulvalene ; ,e) Hexaammineruthenium (III) chloride and f) Potassium ferricyanide . Scan rate = 25 mV s^{-1}

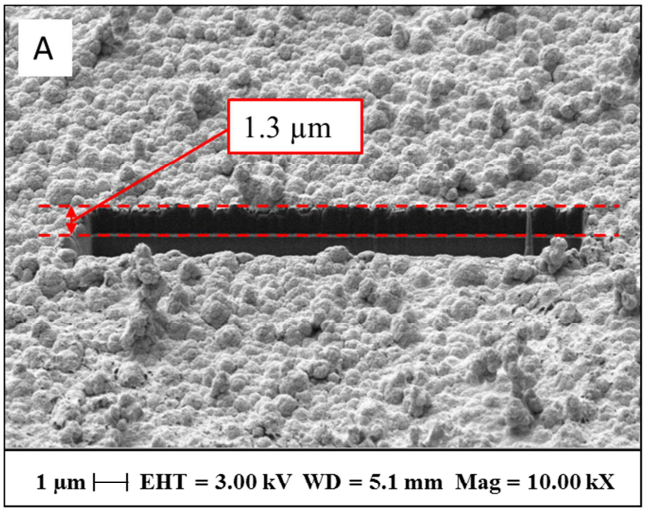

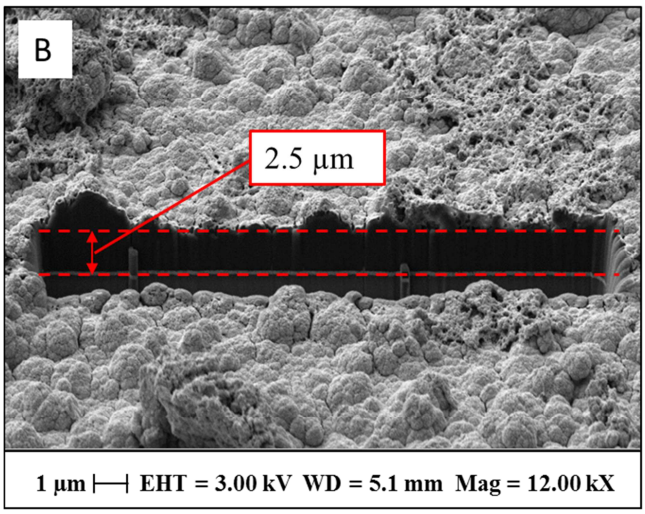

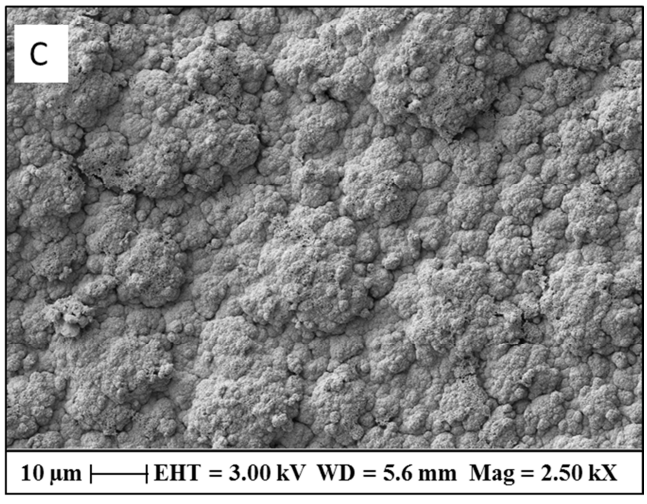

Fig. S6. SEM images of the transversal cut done by FIB for the estimation of the thickness of (A) PPy/mediator and (B) PPy/enzyme membranes. C) SEM image showing the morphology of the PPy membrane surface.